npg

ORIGINAL ARTICLE

Variable optofluidic slit aperture

Stefan Schuhladen[1], Kaustubh Banerjee[1], Moritz Stürmer[2], Philipp Müller[1], Ulrike Wallrabe[2] and Hans Zappe[1]

The shape of liquid interfaces can be precisely controlled using electrowetting, an actuation mechanism which has been widely used for tunable optofluidic micro-optical components such as lenses or irises. We have expanded the considerable flexibility inherent in electrowetting actuation to realize a variable optofluidic slit, a tunable and reconfigurable two-dimensional aperture with no mechanically moving parts. This optofluidic slit is formed by precisely controlled movement of the liquid interfaces of two highly opaque ink droplets. The 1.5 mm long slit aperture, with controllably variable discrete widths down to 45 µm, may be scanned across a length of 1.5 mm with switching times between adjacent slit positions of less than 120 ms. In addition, for a fixed slit aperture position, the width may be tuned to a minimum of 3 µm with high uniformity and linearity over the entire slit length. This compact, purely fluidic device offers an electrically controlled aperture tuning range not achievable with extant mechanical alternatives of a similar size.

INTRODUCTION

Linear slit apertures are used in a wide variety of optical systems including spectrometers and hyperspectral imaging systems[1,2]. In most cases, varying the slit width is essential for optimization of light throughput and resolution for a particular application[3]. The availability of a single variable slit aperture of sufficient resolution and precision allows an optimized slit adjustment for each application without recalibration and thus greatly simplifies a spectroscopic measurement procedure. Alternatively, a laterally scanning slit can be configured so as to replace the need for rotation of the grating in a monochromator or two crossed scanning slits may be employed for line or pixel selection[4].

Existing variable mechanical slit apertures are too bulky for incorporation into miniaturized optical systems[5]. Existing attempts at miniaturization have not reached the required tuning ranges[4]. The technologies of optofluidics provide a lucrative alternative for small-scale tunable systems[6] and we show here how an optofluidic system can be conceived to allow high-precision tuning of a variable slit aperture.

Optofluidics relies on the use of controllably movable and positionable liquid interfaces to realize particular optical functionality. Typically configured using two immiscible liquids in a microfluidic cavity, these fluids are actuated using an approach such as electrowetting-on-dielectrics (EWOD). This fluidic actuation scheme, proposed in 1993[7], creates an electric field in between an electrode and a conductive liquid that is insulated by a thin dielectric film. By varying the applied voltage, the energetically favorable wetting state of the liquid on the insulated electrodes can be adjusted. The process has several advantages such as easy electrical controllability and high reversibility especially with alternative current (AC) voltages[8]. The effect is now well characterized[9,10] and has been successfully applied in different fields such as droplet-based lab-on-a-chip systems[11], electronic displays[12,13], and optofluidics. Two prominent examples for the compact implementation of optofluidic devices are micro-irises[6,14–18] and microlenses[19–21]. Most of these are circularly symmetric optical structures.

We show here how the techniques of optofluidics may be extended to the development of a new component, a variable and repositionable optical slit aperture. This tunable component is designed to scan a highly uniform 100 µm wide slit across a field of 1.5 mm × 1.5 mm in discrete steps; the slit width may be step-wise increased to cover the entire 1.5 mm wide aperture. In addition, for a slit at a fixed position within this field, the slit width may be tuned to a minimum value of 3 µm, relying on the known effect that abutting droplets with the same electrowetting potential do not merge[9,10]. The only previously demonstrated[22] width-tunable optofluidic slit was limited in its minimum width to 160 µm and employed direct current (DC)-electrowetting, which is known to be prone to charge trapping[8,23]. The more reliable AC electrowetting employed here allows reduction of minimum slit width to a few micrometers and considerably enhances both the reconfigurability and performance capabilities of the tunable aperture.

MATERIALS AND METHODS

Concept

The variable slit aperture is a complete optofluidic system on a chip, for which the microfluidic chamber is seen before filling with liquids in Figure 1a; the 'area of interest' is the 1.5 mm × 1.5 mm open field in which the variable slit is positioned. As is shown schematically in Figure 1b, the device functionality is based on the movement of two separate reservoirs of an aqueous opaque fluid (an ink) deposited in the microfluidic chamber and surrounded by an immiscible density-matched transparent oil. Patterned surface layers of Cytop, a highly hydrophobic polymer shown in green in the sketch, define the
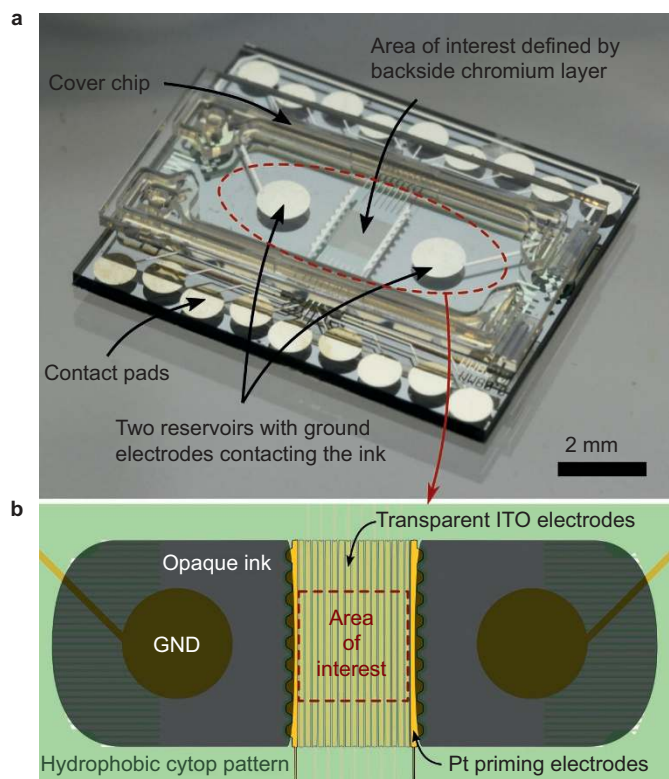
Figure 1 (**a**) Picture of the unfilled adjustable optofluidic slit demonstration chip with attached cover. The slit is formed in the central quadratic transparent area defined by a chromium layer on the bottom side of the chip. (**b**) Top view schematic of the ink-filled device.
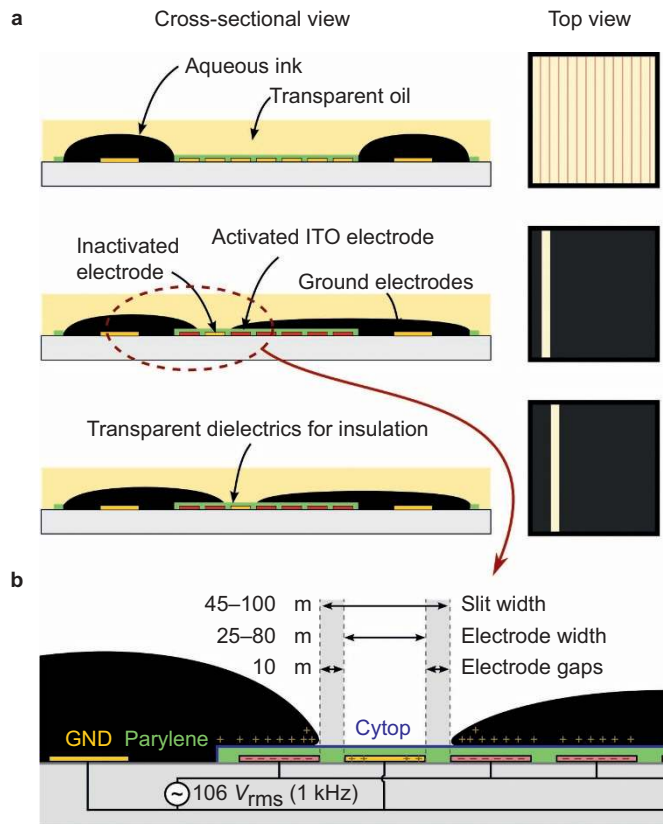

Figure 2 (**a**) Illustration of the electrowetting actuation showing the digital scanning of the slit activation and deactivation of adjacent electrodes. (**b**) Schematic close-up of the electrowetting region showing the electrode gaps and a snapshot of the charge distribution during EWOD actuation.
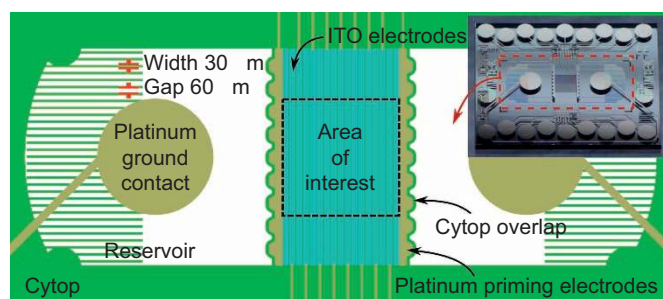

Figure 3 Excerpt of the mask design including the most important design features. The inset shows where the sketched layout is located on the fabricated and diced chip.

initial positions of the opaque aqueous reservoirs for which Pt electrodes provide an electrical ground contact.

In the central 1.5 mm × 1.5 mm open aperture area, 15 structured transparent indium tin oxide (ITO) electrodes, configured as 1.5 mm long stripes and isolated by thin film dielectrics, are then used for precise actuation of the fluids by EWOD. As is illustrated in Figure 2a, application of a voltage to one of the stripe electrodes pulls the opaque ink into the open aperture, where the ink from both reservoirs (left and right) may be independently pulled into the aperture. The gap between the two liquid phase fronts (interfaces) then defines the slit.

As is seen in the detail of Figure 2b, the minimum slit width is achieved when only one central electrode remains unbiased and its width depends on the dimensions of the electrodes and the gaps between them. Devices were fabricated with electrode widths varying from 25 μm to 80 μm; since the spacing between the electrodes was fixed at 10 μm, the minimum optical aperture slit width varied between 45 μm and 100 μm. Due to the high absorption of the ink ($>0.8\,dB\,\mu m^{-1}$), the edge of the slits is a sharp transition and shows no measureable gradient. By reconfiguring the voltages applied to the 15 electrodes, the slit position and width can be set to discrete values and widely varied across the 1.5 mm full aperture.

As we will see in more detail below, electrostatic repulsion between the two aqueous phase fronts keeps these two surface tension stabilized opaque droplets from merging. As a result, the slit width becomes a function of the applied bias and an increase of this bias results in a decrease of slit width that is no longer limited by the structured electrodes. Using this modality, the slit width can be tuned down to about 3 μm.

Design

The optofluidic slit aperture is based on a microfabricated glass chip structured for electrowetting actuation. An excerpt of the mask layout which defines this actuation chip is seen in Figure 3. It shows some of the crucial features of electrode design and here we discuss three important aspects of the electrode configurations essential for reliable slit performance.

(1) Since the coupling between the electrodes and the liquids in the optofluidic chamber is capacitive, the electrodes must be completely covered by an insulating dielectric. Complete insulation requires that this dielectric extends beyond the edge of the electrode

to completely cover its edge, but therefore yielding a gap over which the liquids must be pulled to reach a biased electrode. For that reason, curved finger priming electrodes, as shown in Figure 3 are designed such that the liquid in the filled reservoir slightly overlaps some of the electrode fingers. This priming feature guarantees reliable and reproducible actuation by EWOD.

(2) Small volumes of liquids, in the microliter-range, usually do not form straight liquid phase fronts due to surface energy minimization; however, an optically usable slit aperture requires straight slit sidewalls. To assure a straight liquid interface over the entire 1.5 mm length of the cavity, actuation electrodes were designed to be longer than the intended slit length; this configuration showed good slit interface reproducibility and high linearity of the phase fronts in the area of interest.

(3) The shape and size of the reservoir defined by the structured hydrophobic Cytop layer is also crucial for good performance. An important feature in the design is the arrangement of thin Cytop finger structures at the rear of the reservoir as seen in Figure 2a. With a width of 30 μm and a periodicity of 90 μm, the structures are too small for the meniscus of a large droplet to follow. Thus, the pattern creates a semi-hydrophobic area where the hydrophobicity is a function of the feature sizes (we could call it a wetting metasurface). These finger structures then assist the forward actuation of the liquid front: in the initial state, the Cytop finger structure area is wetted by the ink, but upon actuation the liquid preferably dewets this area, thereby facilitating forward actuation by EWOD.

Micro-fabrication and assembly
The fabrication of the device, as summarized in Figure 4, is based on established wafer level processes[6,24]. Fabrication of the actuation chip, with the electrodes, starts with 500 μm Corning EXG glass wafers coated with 20 nm of ITO. First, platinum (100 nm on the front side) and chromium (50 nm on the back side) metallizations are structured by lift-off. The ITO is then structured by wet etching in an 18% HCl solution at 50 ℃. The vapor deposited Parylene C (5 μm) and the spin coated Cytop (1 μm) are etched in a reactive ion etching unit with O_2 plasma.

Ordyl dry film resist defines the mechanical alignment structures for the cover chip. The cover chips are processed on a 500 μm Pyrex wafer using SU8 lithography, laser cut holes and Cytop dip coating. The devices are manually assembled at the chip level and the cover is affixed by a previously developed stamp and stick epoxy adhesive technique[24]. For the measurements presented in this paper, the chips were characterized without cover. Each reservoir is filled with about 6 μL of ink dosed with 1 wt% Na_2SO_4 and 1 wt% of the surfactant Tween20. The surrounding medium is Dow Corning 200 Fluid, a 50 cSt silicone oil.

RESULTS AND DISCUSSION
Aperture scanning
By applying an appropriate time-dependent voltage sequence on the electrode array, the position of the slit aperture may be scanned across the 1.5 mm field region. Recalling the schematic representation of the electrode configuration in Figure 2, we see that the slit aperture width may also be varied in discrete steps: a minimum width of 100 μm is attained with only one unbiased electrode separating the two fluid fronts. By increasing the number of unbiased electrodes, the slit aperture width may then be increased in steps of 100 μm.

The scanning performance of the slit aperture is shown in Figure 5: an AC driving voltage of 106 V_{rms} at a frequency of 1 kHz was applied consecutively to the different actuation electrodes allowing a 100 μm wide slit to be scanned across the central field area of 1.5×1.5 mm^2. A frequency of 1 kHz avoids oscillations of the liquid edge due to the
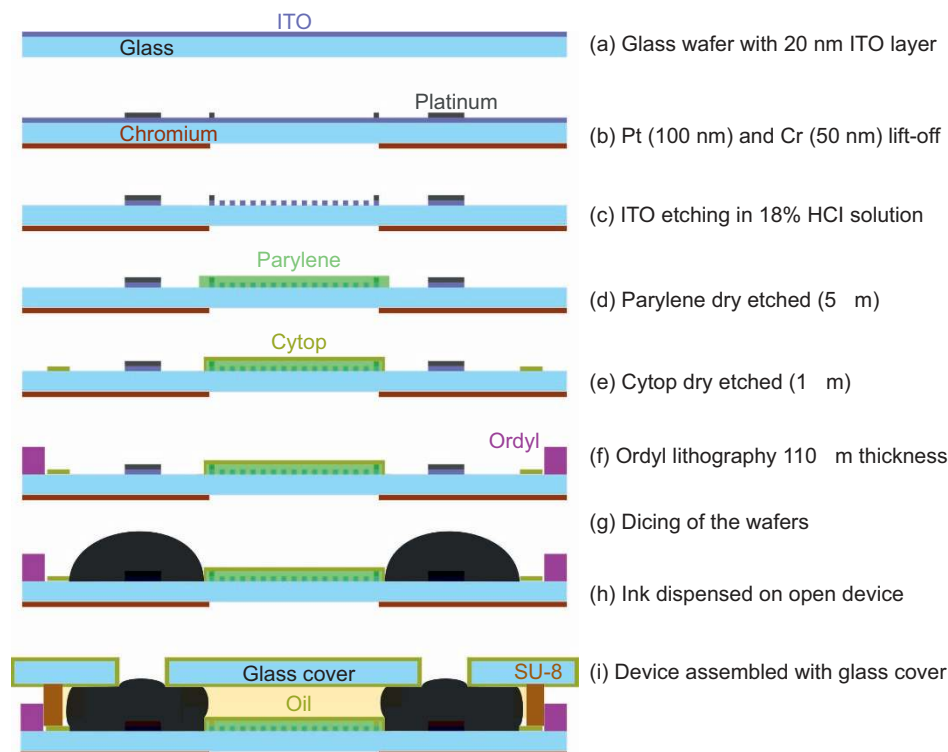

Figure 4 Illustration of the fabrication process: standard cleanroom processes are used to deposit and pattern thin films and permanent dry film structures for alignment. Dispensing and cover assembly are completed on chip level.
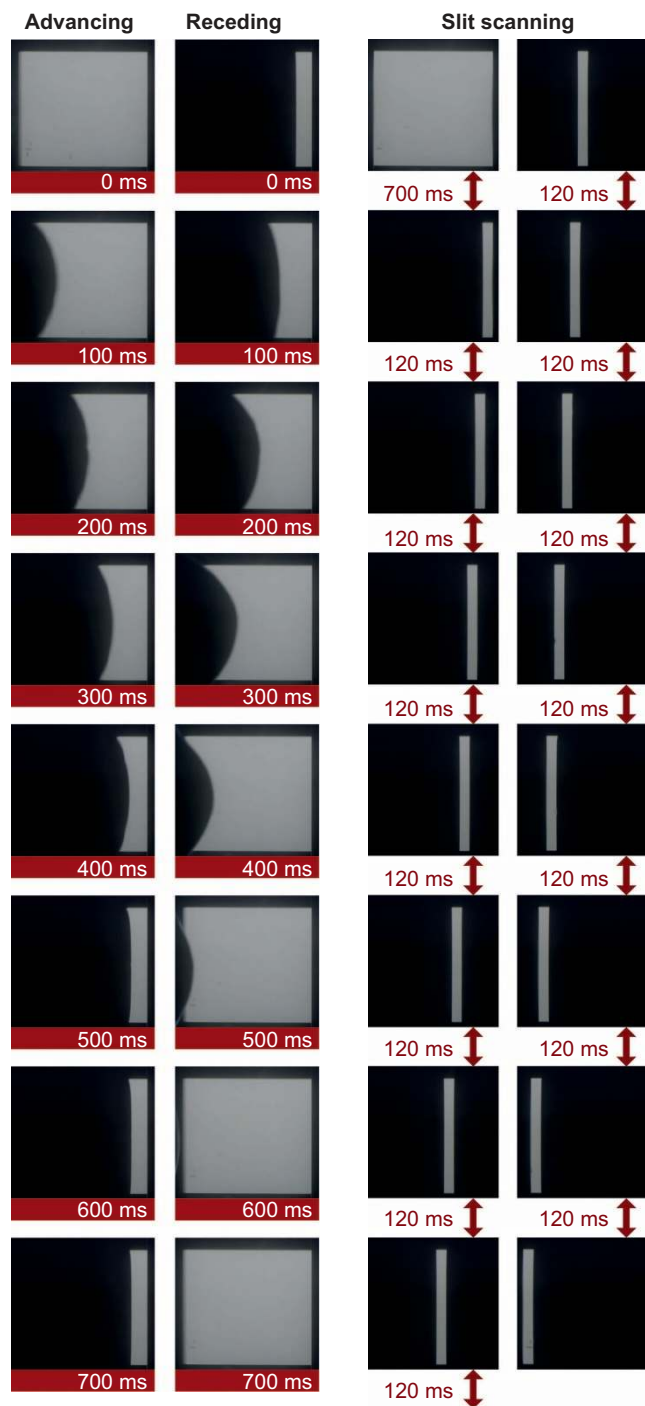
Figure 5 Left side: image series showing the advancing and receding of one liquid front for analysis of the maximal switching times for 106 V_{rms} at 1 kHz. Right side: images of different switching states with the measured maximal switching times between the states at the same conditions.

Figure 6 Evolution of the advancing (triangles up) and receding (triangles down) liquid front position over time for 106 V_{rms} at 1 kHz, as observed for both sides of the slit and for the maximal actuation distance of 1.4 mm. The measured time constants for 10%–90% transition are indicated.

based on analysis of individual frames of the video using scripted image processing, are shown in detail in Figure 6.

Using the 10%–90% rise and fall times as benchmarks for the opening and closing of the entire field, we see that, for a liquid front from the left, the closing time is about 350 ms and the opening time is about 370 ms. For the liquid front moving from the right, the time constants for closing are about 25 ms faster and for opening about 20 ms slower; thus the total times required for forward and back-actuation are about the same on both sides. The difference for the time constants for actuation from the two sides can be explained by small variations in the amount of dispensed liquid in the reservoirs on both sides. A larger amount of liquid eases forward actuation (closing) but hinders passive backward (opening) actuation.

Once a slit aperture has been attained by 'closing' the liquid fronts, the slit position can be switched by applying a voltage sequence to the electrode array. As is seen in the right side of Figure 5, the slit aperture can be scanned across the entire field, with a switching time constant of about 120 ms. This time constant was again derived from the video sequence, and is an approximation: each switching step required about six frames of the video, corresponding to 120 ms. Detailed examination of the liquid phase fronts defining the slits confirmed that the slit profile is very straight over the entire 1.5 mm field region, as the liquid front is defined by the long, straight electrode. A video showing these actuation sequences in real time is available in the Supplementary Information.

As mentioned above, the width of the scanned slit aperture is defined by the structure (width) of the electrodes. In the data shown in Figure 5, an electrode width of 80 µm and an inter-electrode gap of 10 µm resulted in a slit width of 100 µm. As shown in Figure 7a, smaller slit widths, down to an electrode width of 25 µm at a constant inter-electrode gap of 10 µm, are also realizable. These smaller widths were successfully demonstrated and showed the expected minimum slit widths of 45 µm. As the mask and lithography quality define the realizable electrode and spacing widths, even smaller slit widths may be defined. The functionality of the semihydrophobic Cytop fingers is demonstrated in Figure 7b: The liquid starts to dewet from the fingers as soon as it is moving forward, which facilitates the actuation by EWOD. This can be understood from the fact that a liquid volume

actuation frequency[8], as these are observed for frequencies below 100 Hz for the liquid combination. The left side of the figure first shows an image sequence resulting when switching from full field (completely open field aperture) to slit mode. Both the advancing (ink moves into the aperture) and the receding (ink retracts from the aperture) sequences for movement of the liquid front across the full aperture length are analyzed. The dynamics of this movement,
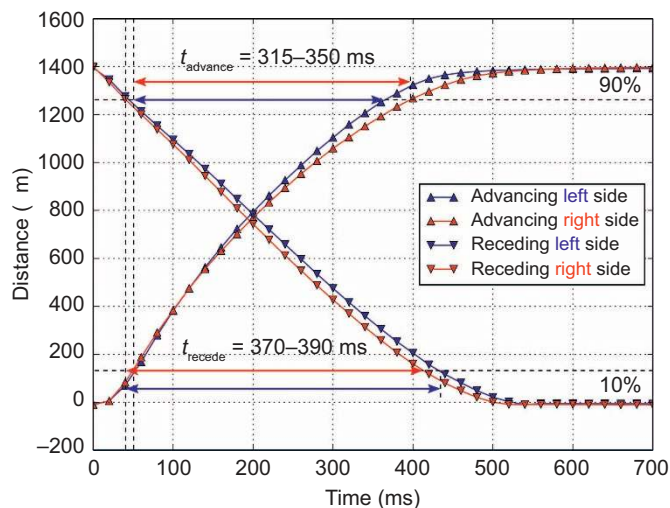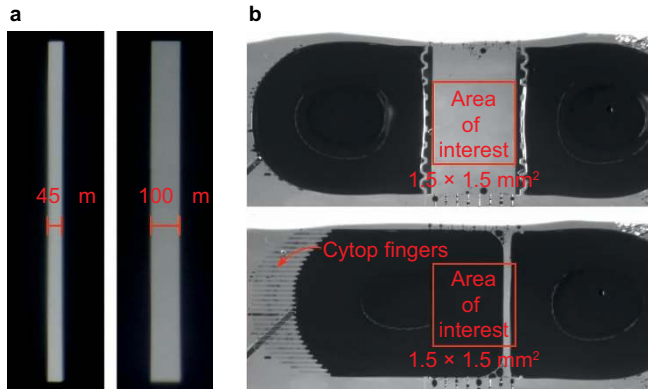
Figure 7 (**a**) Scanning slits down to a slit width of 45 μm formed by electrowetting on structured electrodes of widths down to 25 μm. (**b**) Images showing the dewetting of the semi-hydrophobic Cytop fingers that supports forward actuation.

which is pinned on a strongly hydrophilic surface will resist to a movement away from this pinning site, whereas, if no pinning sites are present, the liquid can advance freely.

Slit width tuning

The second modality of the variable slit aperture is the tuning of the slit width for a slit in a fixed position. So long as the surface tension is not too low, two droplets actuated by electrowetting at the same electrical potential will not merge if they interact with each other during actuation. Even without structured electrodes, liquids actuated toward each other from two equally sized reservoirs establish a straight gap in between them, located at the position where the liquids approach each other but are repelled electrostatically. Once two liquid phase fronts are in this state, the width of the slit can be tuned by varying the applied EWOD voltage.

The variation in the lateral position of the slit was evaluated using the structured electrode design of the aperture scanning device. As all electrodes are activated, the position of the slit is not fixed, but the experiments still showed quite reproducible slit positions with maximal variations of only ±20 μm, if the slit is formed on an unstructured electrode. The lateral position and orientation is however precisely defined, if the slit is formed on top of an electrode gap. In this case, the electrode gap width limits the minimal slit width to which the slit can be tuned.

The transition times from the 100 μm silt to the equilibrium state with all electrodes turned on varies slightly depending on the applied initial tuning voltage, but for 106 V_{rms} the transition is completed within 250 ms.

Using a single electrode structure, the slit width was measured using an inverted microscope with 1000× magnification, resulting in an estimated measurement accuracy of ±0.2 μm. The images of the slit recorded by a digital camera in combination with a calibrated reference slide yielded the slit widths as shown in Figure 8; images of the slit for a subset of measurement points are also shown as is an expanded view of the shaded narrow-slit region. The measured slit widths, ranging from 61.8 μm to 2.8 μm, are far smaller than any previously reported minimum width values, namely 160 μm for an EWOD actuated slit[22]. For this measurement, the curve fit of the width was a function of the rms (root mean square) voltage V_{rms}, is of the form
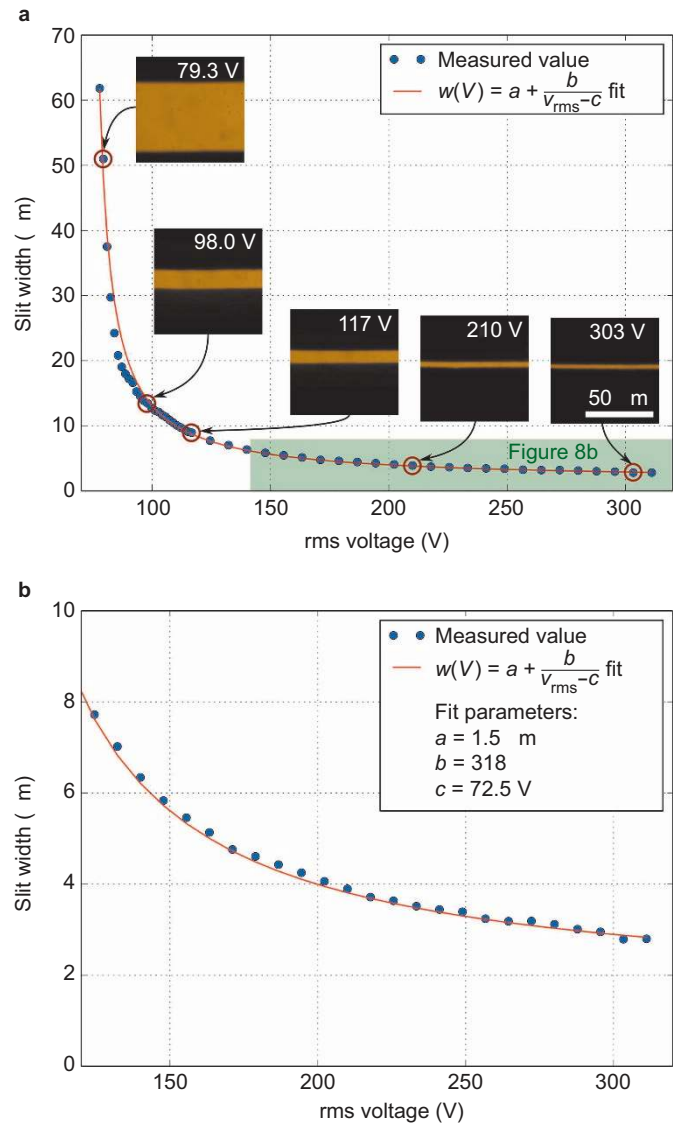
$$w(V) = a + \frac{b}{V_{rms} - c} \qquad (1)$$

Figure 8 (**a**) Analog tuning of the slit in a central position with the according evaluated microscope images. Reciprocal fit with rms voltage at 1 kHz. (**b**) Excerpt of the graph showing a clear trend for the slit widths at high voltages.

with the fit parameters $a = 1.5$ μm, $b = 318$, and $c = 72.5$ V, showing that the reciprocal relationship between applied voltage and slit width holds over a large voltage range. As the detail in Figure 8b indicates, this reciprocal relationship holds for high voltages, suggesting that even smaller slit widths are possible for higher applied bias. The limitation will be dielectric breakdown of the surface layers.

The measured data show that slit widths well below 10 μm can be set with very high precision; the small variations of the measurement points around the fitting curve Figure 8b result from the limited resolution of the optical microscope used to measure the slit width. All slits within the plotted range showed parallel edges over their full length.

System application

One well-established form of optical instrumentation requiring an accurate slit aperture is the spectrometer, for which the scanning slit is a key component which is used to select the different bands of the spectrum. We demonstrate that this complex functionality can be fully

realized for a spectrometer using the optofluidic slit aperture. Figure 9a and 9b shows a schematic diagram and photograph of the experimental setup. The slit aperture is placed at the position of the first diffraction order of a transmission grating (500 lines mm^{-1}) which is illuminated by a white light source. To reduce the sensitivity of the setup to the position of the detecting fiber, the light transmitted through the slit aperture is first collected by a homogenizing rod before it is directed to a fixed spectrometer at the bottom of the figure. The tunable slit aperture was then scanned across the spread spectrum emerging from the grating. Figure 9c shows the measured spectral bands for all 16 positions of the 100 μm slit, normalized to the peak value of the band with the maximum intensity. The graph also shows

the normalized measured spectrum for a fully opened slit device (full 1.5 mm × 1.5 mm field). As expected, this spectrum matches the sum of the single bands indicated by the red dotted line very well.

This simple setup shows that the tunable optofluidic slit aperture can be used to scan over an entire spectrum of interest using a system with no mechanically moving parts; no rotation or mechanical translation of a fixed slit is required. A comparison with a fixed mechanical slit showed that the slight asymmetry of the selected bands is not induced by the slit but is due to misalignment of the setup and limited grating quality. Smaller slit widths and/or a lower grating period would result in a tunable monochromator with a smaller resolution bandwidth.
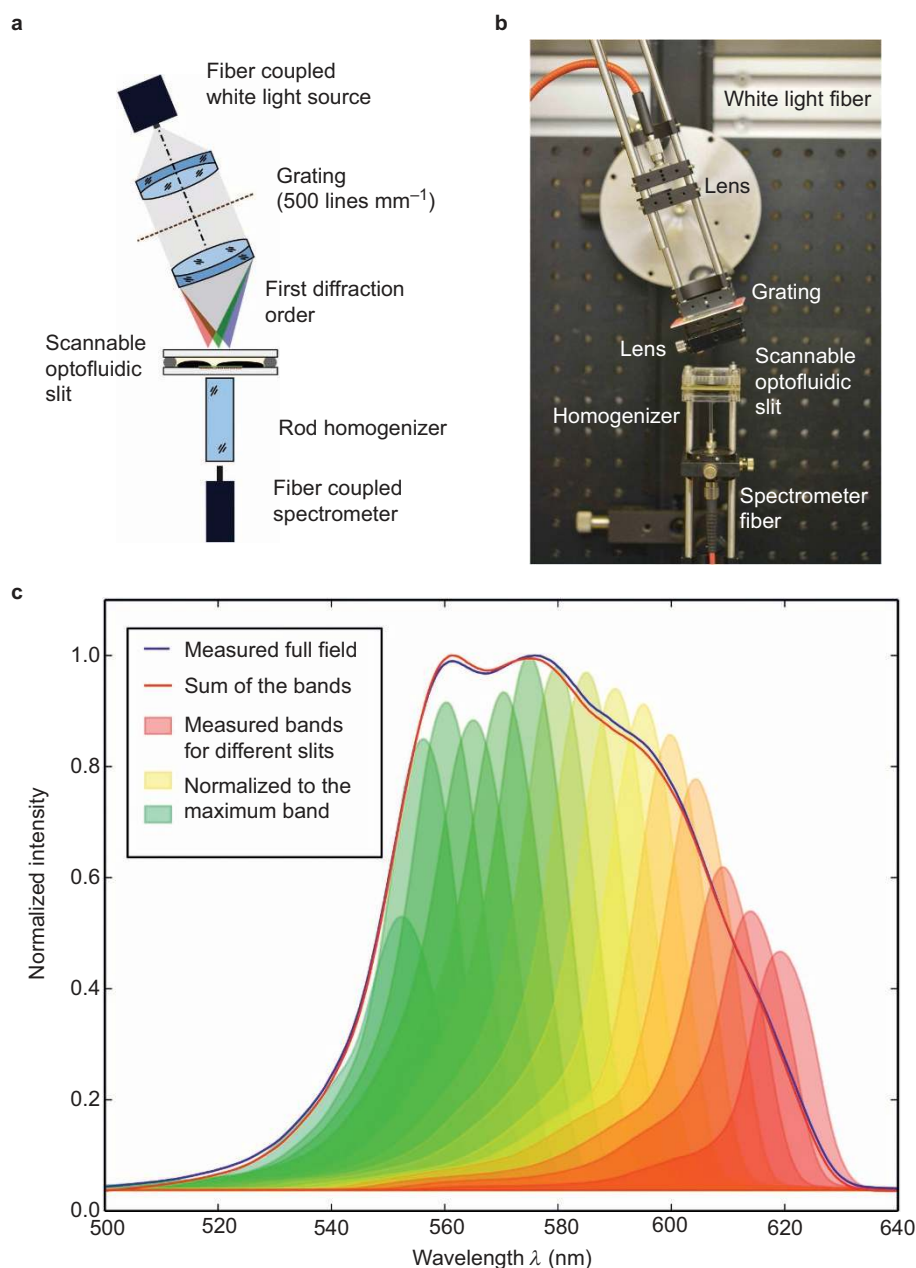

Figure 9 (**a**) Schematic and (**b**) photograph of the band-selector setup. The scanning slit is positioned in the first diffraction order of a grating illuminated by a collimated white light source. The transmitted spectrum is evaluated by a spectrometer via a fiber coupled homogenizer. (**c**) 16 bands of the full spectrum can be selected by different slit positions. The single bands sum up to the full spectrum.

CONCLUSION

We have shown that an optofluidic tunable slit aperture based on AC electrowetting represents a unique and highly versatile tool for the formation of small repositionable slits of variable width. Slit widths ranging from more than 1 mm down to 45 μm can be digitally set with dimensions defined by micro-structured transparent ITO electrodes. These slits can also be laterally translated for applications such as spectrometers in which a specific spectral feature is to be selected. In addition, for a single slit, widths down to about 3 μm can be set by voltage tuning, providing even further flexibility for this highly functional optofluidic device.

ACKNOWLEDGEMENTS

1   Czerny M, Turner A. Über den Astigmatismus bei Spiegelspektrometern. *Zeitschrift für Phys* 1930; **61**: 792–797.
2   Lu G, Fei B. Medical hyperspectral imaging: a review. *J Biomed Opt* 2014; **19**: 010901.
3   Lerner JM. Imaging spectrometer fundamentals for researchers in the biosciences – a tutorial. *Cytom Part A* 2006; **69A**: 712–734.
4   Chronis N, Okandan M, Baker M, Lee LP. A 2-D translational pinhole formed by two orthogonally moving micro-slits. Digest of Technical Papers – The 13th International Conference on Solid-State Sensors, Actuators and Microsystems, Transducers '05; 5–9 June 2005; Seoul, South Korea; 2005, pp. 1022–1025.
5   Vuilleumier R, Kraiczek K. Variable-entrance-slit system for precision spectrophotometers. *Sensor Actuat A Phys* 1995; **50**: 87–91.
6   Müller P, Feuerstein R, Zappe H. Integrated optofluidic iris. *J Microelectromech Syst* 2012; **21**: 1156–1164.
7   Berge B. Electrocapillarité et mouillage de films isolants par l'eau. *C R Acad Sci II* 1993; **317**: 157–163.
8   Li F, Mugele F. How to make sticky surfaces slippery: contact angle hysteresis in electrowetting with alternating voltage. *Appl Phys Lett* 2008; **92**: 244108.
9   Quilliet C, Berge B. Electrowetting: a recent outbreak. *Curr Opin Colloid Interface Sci* 2001; **6**: 34–39.
10 Mugele F, Baret JC. Electrowetting: from basics to applications. *J Phys Condens Matter* 2005; **17**: R705–R774.
11 Abdelgawad M, Wheeler AR. The digital revolution: a new paradigm for microfluidics. *Adv Mater* 2009; **21**: 920–925.
12 Hayes RA, Feenstra BJ. Video-speed electronic paper based on electrowetting. *Nature* 2003; **425**: 383–385.
13 Heikenfeld J, Drzaic P, Yeo JS, Koch T. A critical review of the present and future prospects for electronic paper. *J Soc Inf Disp* 2011; **19**: 129–156.
14 Murade CU, Oh JM, van den Ende D, Mugele F. Electrowetting driven optical switch and tunable aperture. *Opt Express* 2011; **19**: 15525–15531.
15 Chang JH, Jung KD, Lee E, Choi M, Lee S *et al*. Variable aperture controlled by microelectrofluidic iris. *Opt Lett* 2013; **38**: 2919–2922.
16 Li L, Liu C, Ren H, Wang QH. Adaptive liquid iris based on electrowetting. *Opt Lett* 2013; **38**: 2336–2338.
17 Yu CC, Ho JR, Cheng JWJ. Tunable liquid iris actuated using electrowetting effect. *Opt Eng* 2014; **53**: 057106.
18 Schuhladen S, Banerjee K, Stuermer M, Mueller P, Wallrabe U *et al*. Scannable optofluidic slit. 2014 IEEE Photonics Conference, 12–16 October 2014; San Diego, CA, USA; 2014, pp. 568–569.
19 Kuiper S, Hendriks BHW. Variable-focus liquid lens for miniature cameras. *Appl Phys Lett* 2004; **85**: 1128–1130.
20 Hao C, Liu Y, Chen X, He Y, Li Q *et al*. Electrowetting on liquid-infused film (EWOLF): complete reversibility and controlled droplet oscillation suppression for fast optical imaging. *Sci Rep* 2014; **4**: 06846.
21 Simon E, Berge B, Fillit F, Gaton H, Guillet M *et al*. Optical design rules of a camera module with a liquid lens and principle of command for AF and OIS functions. *Proc SPIE* 2010; **7849**: 784903.
22 Li L, Liu C, Wang MH, Wang QH. Adjustable optical slit based on electrowetting. *IEEE Photonics Technol Lett* 2013; **25**: 2423–2426.
23 Nanayakkara YS, Perera S, Bindiganavale S, Wanigasekara E, Moon H *et al*. The effect of AC frequency on the electrowetting behavior of ionic liquids. *Anal Chem* 2010; **82**: 3146–3154.
24 Müller P, Kopp D, Llobera A, Zappe H. Optofluidic router based on tunable liquid-liquid mirrors. *Lab Chip* 2014; **14**: 737–743.

Supplementary information for this article can be found on the *Light: Science & Applications'* website (http://www.nature.com/lsa).